

# TCAD Simulation Methodology for 3-D Advanced Electro-Physical and Optical Analysis

Patrik Príbytný, Marián Molnár, Aleš Chvála, Juraj Marek, Miroslav Mikolášek, and Daniel Donoval

Institute of Electronics and Photonics, Slovak University of Technology in Bratislava

Bratislava, Slovakia

Email: patrik.pribytny@stuba.sk

**Abstract**—This is first demonstrated using a full 3-D approach, where a global model includes a part of a solar cell with a textured surface. Due to device complexity, many of them cannot be simulated in the full 3-D setup within a reasonable amount of time. Therefore, derived solutions are proposed, which are based on the combined-mode setup coupling the 3-D TCAD model of the solar cell to a “standard” TCAD (2-D or 3-D) model of the active device. We propose a smart coupling between the device and the package that combines the speed and accuracy of mixed-mode simulation assuming additional 3-D effects.

**Keywords**—solar cell, TCAD model, 3-D effects, back contact, heterojunction

## I. INTRODUCTION

The photovoltaic community has demonstrated and proposed a wide variety of solar cell structures using a wide range of photovoltaic semiconductor materials. Numerical modeling has proved to be a valuable tool in understanding the operation of these devices. 1-D simulations are usually adequate for conventional geometry solar cells. 2-D effects can become important in conventional geometry solar cells and many high efficiency cell designs require 2-D simulations or even 3-D simulations. The 3-D simulators are nowadays essential in semiconductor device modeling in order to study fluctuation effects. To take into account these effects it is necessary to perform statistical studies, which have a high computational cost. The resolution of the linear systems generated by the discretization of partial differential equations is the most time-consuming part of the simulation process. The parameters of electro-physical and optical models and the boundary conditions of used equations can be very complex. They depend on microscopic physics and the structure of the device. Device simulator SDevice [1] allows simulation of electrical characteristics for selected combinations of transport equations and physical models. These models provide the potential to simulate a wide spectrum of semiconductor devices.

We propose a smart coupling between the device and the package that combines the speed and accuracy of mixed-mode simulation assuming additional 3-D effects. This approach involves the coupling of optical and electro-physical simulations in the package. The basic approach considers multiple connections of several devices to multiple parts located on the cell. To bring locally generated current information on the cell into the electro-physical and optical

simulation of the device, a possible solution involves the splitting of the single node into several nodes, and connecting each of them to a single 2-D or 3-D solar cell. Therefore, the simulation requires solving the drift-diffusion and the Poisson equations in several solar cells instead of just one, and the carrier continuity equation is solved in the solar cell as in the previous case. The partitioning of the original problem into a multiple mixed-mode approach seems to be the most attractive solution, since it couples the accuracy of TCAD simulation of the device embedded into a solar cell and a short simulation time, while preserving information on the non-uniformity of generated current with self-consistent coupling to TCAD elementary devices.

## II. STRUCTURE AND MODEL DESCRIPTION

Fig. 1 shows cross-section of the solar cell structure with the implanted  $N^+$  buffer layer used in our simulations. The a-Si:H(p) p-contact is formed as a point contact and the a-Si:H(n) emitter represents the area around this point contact. The a-Si:H(n)/c-Si(p) emitter interface is passivated by a 5 nm thick layer of a-Si:H(i). A 1  $\mu\text{m}$  thick implanted  $N^+$  buffer layer is formed in the silicon substrate of the emitter interface. Thus the layer sequence of the emitter structure is as follows: a-Si:H(n)/a-Si:H(i)/c-Si( $N^+$ )/c-Si(p). In the sequel this emitter structure is labeled as a-Si:H(n)/c-Si(p) for simplicity reasons. The results obtained on BC-SHJ with  $N^+$  buffer layer were compared with an identical structure without the  $N^+$  buffer layer. In the simulated model of both structures a 300  $\mu\text{m}$  thick p-type crystalline silicon (c-Si) wafer with concentration  $\sim 10^{15} \text{ cm}^{-3}$  is passivated with  $\text{Si}_3\text{N}_4$  (70 nm) at the front surface. The electron and hole lifetimes for c-Si are set to 1 ms. The rear a-Si:H(p) p-contact and a-Si:H(n) emitter n-contact are placed at the bottom of the wafer, both with thicknesses of 20 nm. For a-Si:H layers, the critical parameters such as the band gap, doping (conductivity), energy distribution of the exponential band tails, and the Gaussian distribution of mid-gap dangling bonds states are chosen based on reference [2, 3] and tuned to fit the measured optoelectronic properties of the deposited a-Si:H layers. Parameters of the model are listed in Table 1. The conduction band offset of 0.15 eV and defect states density of  $10^{12} \text{ cm}^{-2}$  were set as default values at the a-Si:H(n)/c-Si(p) interface. In the simulation, these parameters were varied to investigate the impact of the heterointerface properties on the output

performance. The a-Si:H(p)/c-Si(p) contact properties were modeled without defect states.

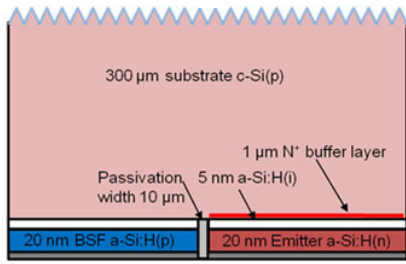


Fig. 1 Cross-section of the simulated structure of BC-SHJ with  $N^+$  buffer layer. The rear a-Si:H(p) p-contact is a point contact surrounded by an a-Si:H(n) emitter.

The default width of the p-point contact is 0.6 mm. The default distance between two p-contacts is 0.62 mm. The area between the p-contacts represents the emitter, which is isolated from the p-contact by the isolation gap with a width of 10  $\mu\text{m}$ . In the simulation, the width of the p-contact was fixed and the area of the emitter contact was parameter.

Three basic semiconductor equations were solved the Poisson equation, electron and hole continuity equations together with the drift-diffusion model Auger and Shockley-Read-Hall recombination's were also taken into account for the crystalline silicon wafer. For a-Si:H(n)/c-Si(p) emitter heterointerface a thermionic emission model was applied in which the distribution function of the interface defects is modeled by two Gaussian functions, one for acceptor and one for donor type defects. An AM1.5G solar spectrum was used for the optical generation to simulate the  $J-V$  curve under standard one-sun illumination conditions at intensity of 100  $\text{mW}/\text{cm}^2$ .

### III. SIMULATION METHODOLOGIES

The light absorbing capability of a solar cell is greatly enhanced when its surface is textured. When the cell surface is rough, rather than planar, it is less reflective, and a higher proportion of the incident radiation can be utilized in the device. As a result, higher cell efficiency is achieved. For wafered solar cells in particular, the reduction of front surface reflection, rather than the improvement of light trapping, is the most effective means to enhance the cell short circuit current. We created new approach with combination 3-D surface texture of solar cell with electro-physical full 3-D model (Fig. 2).

Textures fulfill two main tasks: (i) to reduce reflection at the front surface and (ii) to improve absorption in the solar cell bulk by increasing the effective path length of the light in the solar cell. The mechanism behind the reflection reduction is a multiple reflection of the incident light, as sketched in Figure 2. When interacting with the texture, some light is transmitted into the solar cell and some light is reflected. The reflected light may interact with the texture again, depending on the direction of reflection. It is a special feature of pyramidal textures that all light is reflected twice or more often. In this way, a significantly larger fraction of light enters the solar cell

compared to a planar surface. Weighted over the solar spectrum, a planar silicon wafer reflects 36% of the incident light, whereas a wafer with upright pyramids reflects only 12%.

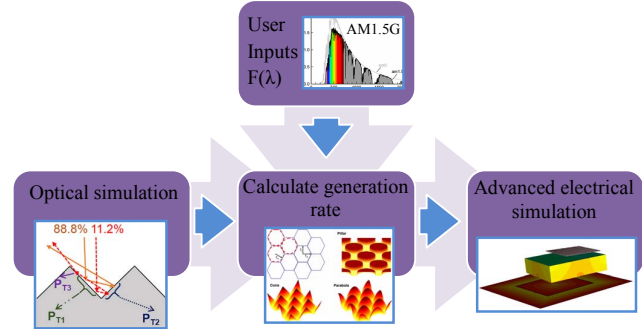


Fig. 2 The solar cell workflow starts with optical simulations in Sentaurus. Taking the solar spectrum into account, the generation rate is calculated from the optical absorption and used as a source in the subsequent electrical simulation in device to calculate the quantum efficiency [4, 5].

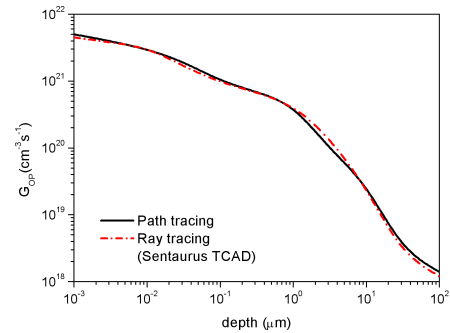


Fig. 3 Simulated 1-D generation profile using the path 3-D method (black curve). Ray tracing results obtained with standard Sentaurus TCAD methodology [6].

The results from our new optical simulations were compared with a ray tracing calculation using Sentaurus TCAD (Fig. 3) and we found only negligible differences between the calculated generation profiles.

To bring locally generated current information on the cell into the electro-physical simulation of the device, a possible solution is the splitting of the single node into several ones, each of them being connected to a single 2-D or 3-D solar cell. Fig. 4 shows a schematic of the enhanced combined-mode approach. In our new setup, the single node is discretized into three nodes: one is placed on the surface, one fills the light area, and one is located at the interface between contact and silicon. Therefore, the simulation requires solving the drift-diffusion and the Poisson equations in three solar cells instead of one, and carrier continuity equation is solved in the solar cell as previously.

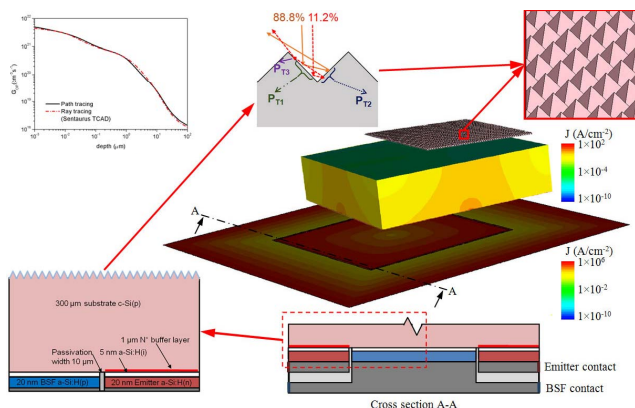


Fig. 4 Full 3-D approach, where global model includes a part of solar cell with textured surface. Cross-section of the simulated structure of BC-SHJ with implanted buffer layer. The rear a-Si:H(p) p-contact is a point contact surrounded by an a-Si:H(n) emitter.

In realistic devices (such as solar cells), the active area consists of many (sometimes many thousands) cells or stripes, which make a full 3-D TCAD approach almost impracticable. A simpler setup can be built to overcome this problem. This solution consists of splitting the full simulation model into a 3-D TCAD model of the package (including simplified die) and a “classical” TCAD description of the device (a “classical” TCAD model here refers to an elementary cell in 2-D or 3-D, depending on the device structure itself). The two parts are connected to each other in “combined-mode” setup [7]. The “classical” TCAD device model is based on a 2-D cross section of a cell. The combined-mode setup is built to allow current density and optical generation exchange between the package and device via electric and optoelectric nodes. The package setup includes part of the solar cell, the discrete device package and simplified silicon die (Fig. 5).

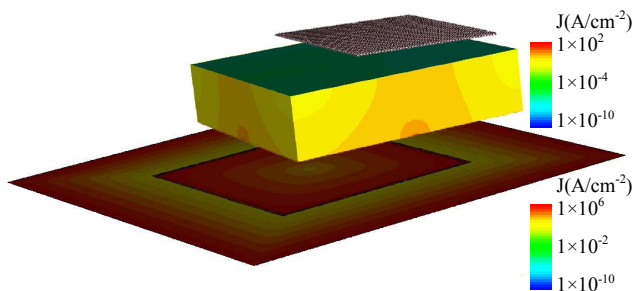


Fig. 5 Full 3-D simulation approach for discrete solar cell device including optical model for texture simulated employing Sentaurus Device.

#### IV. FULL 3-D MODELING

The full 3-D modeling provides accurate results (parameters of solar cell) and a complex interaction of current distribution on the device electrical behavior. However, such an approach can be applied to the part of cell alone, but it is difficult to apply to the full system. Building a TCAD model from a complex device design (thousands of cells or stripes) would easily lead to several millions of mesh nodes without

even getting a sufficiently accurate grid. To bring local generated current information on the cell into the electro-physical simulation of the device, a possible solution is the splitting of the single node into several ones, each of them being connected to a single 2-D or 3-D solar cell. The partitioning of the original problem into a multiple mixed-mode approach seems to be the most attractive one, since it couples the accuracy of TCAD simulation of the device embedded into a solar cell and a short simulation time, while preserving information on the non-uniformity of generated current with self-consistent coupling to TCAD elementary devices.

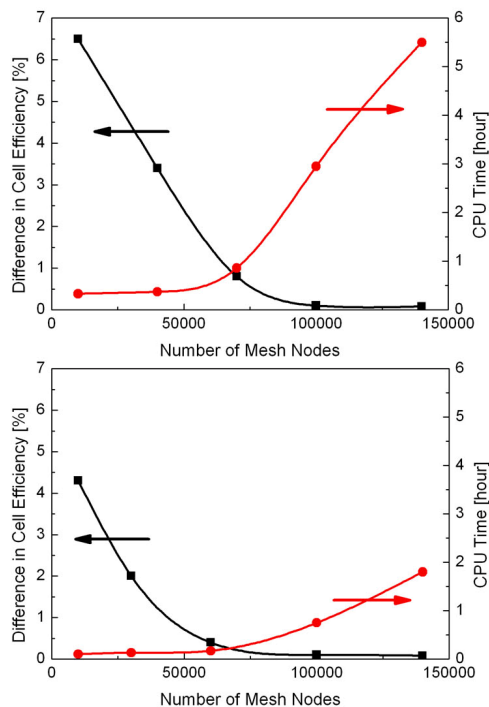


Fig. 6 Simple study on meshing strategies: accuracy versus CPU time trade-off. Top: Full 3-D simulation [8], Bottom: combined 2-D/3-D simulation approach.

Theoretically, the more dense mesh provides more accurate simulation results. However, practically, a good mesh is refined sufficiently to provide the required accuracy but not over refined to consume a reasonable simulation time. Fig. 6 shows an example of a test. When the total number of mesh nodes is only 20000, the simulation result is inaccurate with an error of more than 6.5%. On the other hand, when there are more than 100000 nodes, the simulation time becomes too long. Neither of them is considered as a good approach. In this particular case, a good trade-off is achieved with a locally refined mesh with 30000 nodes, which gives a 0.8% error and allows the simulation to finish within 60 minutes of CPU time.

Different modeling approaches already exist, which typically rely on compact models. However, these approaches neglect the spatial nature of the device of the electrical and optical parameters, which can play an important role in the application. In this paper, a 3-D simulation analysis of the solar cell includes a complete description of the semiconductor structure in terms of optical profile, and an electro-physical

modeling of the device using drift-diffusion transport. We present a 3-D simulation study of BC-SJH on p-type substrate with an incorporated implanted  $N^+$  buffer layer in the emitter structure. The simulation study is done with intention to show possible compensation of the negative effect of defect states at the heterointerface and to attain a low sensitivity of  $V_{OC}$  on the interface quality with additional 3-D effects (Fig. 7) [9].  $V_{OC}$  and  $\eta$  plotted as functions of the  $N^+$  buffer layer doping concentration ( $N_{buff}$ ). To fully utilize the potential of SHJ and BC-SJH solar cells, the study and optimization of emitter amorphous silicon/crystalline silicon heterointerface was identified as the most important issue [10, 11, 12, 13]. Results are compared with a solar cell in published results [9].

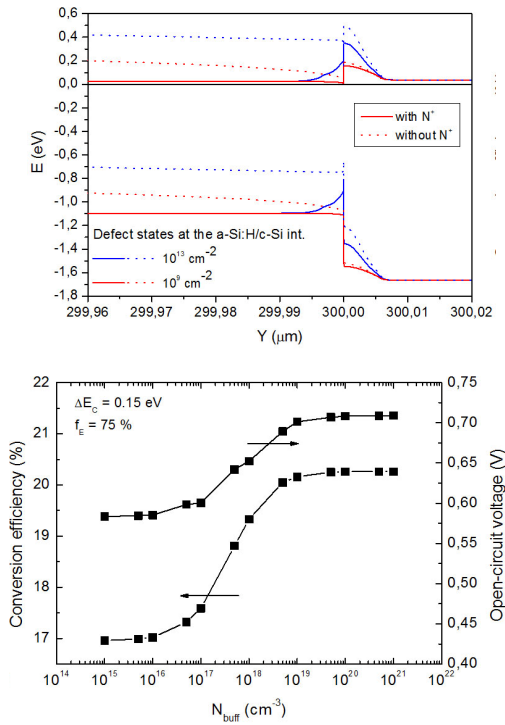


Fig. 7 Top: Calculated energy band diagram of the emitter heterointerface for BC-SJH with and without  $N^+$  buffer layer and  $N_{ii} = 10^9$  and  $10^{13} \text{ cm}^{-2}$ . Bottom: Calculated conversion efficiency and open-circuit voltage for structure with  $N^+$  buffer layer plotted as functions of  $N_{buff}$ .

## V. CONCLUSION

In this paper, TCAD simulations of solar cells including accurate modeling of electro-optical properties were performed. Due to a device complexity many of them cannot be simulated in the full 3-D setup in the reasonable time. Therefore derived solutions based on the combined-mode setup coupling the 3-D TCAD model of the solar cell to a “classical” TCAD (2-D or 3-D) model of the active device are proposed. The latter methodology provides both good accuracy with respect to full 3-D modeling and short simulation time ( $6 \times$  faster than full 3-D when feasible). Very good agreement between the new approach in the 3-D simulation and published results [2] confirms the validity of the proposed methodology. The advantages of the proposed method are in the high speed of simulation and simplicity of implementation for complete, high complexity structure analysis. The analysis of optical and

electrical behavior can help during the design and optimization of parameters and geometry from semiconductor layers, metallization, package, and up to textured surface.

## ACKNOWLEDGMENT

This work was supported in part by Grant VEGA 1/0491/15, and the ENIAC JU project no. 621270/2013 eRamp supported by Ministry of Education, Science, Research and Sport of the Slovak Republic.

## REFERENCES

- [1] TCAD Sentaurus User Manual, Version J-2014.09, Synopsys, San Jose, CA, USA, 2014.
- [2] J. Haschke, N. Mingiruli, B. Rech: “Progress in Point Contacted Rear Silicon Heterojunction SolarCells”, Silicon PV 2012, 116-121.
- [3] C. Lee, H. Efsthadiadis, et, all: “Two-dimensional Computer Modeling of Single Junction a-Si:H solar Cells”, PVSC, 34th IEEE, 2009.
- [4] S. C. Baker-Finch, K. R. McIntosh, “Reflection of normally incident light from silicon solar cells with pyramidal texture”, Progress in Photovoltaics, vol. 19, 2011, pp. 406-416
- [5] R. Dewan, S. Fischer, V B. Meyer-Rochow, Y. Ozdemir, S. Hamraz, and D. Knipp, “Studying nanostructured nipple arrays of moth eye facets helps to design better thin film solar cells”, Bioinspir. Biomim. 7 016003 doi:10.1088/1748-3182/7/1/016003, 2012.
- [6] Sentaurus, March 2010 edition, Synopsys Inc., Mountain View, CA, 2008.
- [7] P. Pribytny, M. Molnar; A. Chvala; J. Marek; M. Mikolasek; D. Donoval, “TCAD simulation methodology for 3-D electro-physical and optical analysis”, ASDAM 10th, IEEE, 2014.
- [8] TCAD Sentaurus application note 2014, <<https://solvnet.synopsys.com/retrieve/039602.html>>.
- [9] M. Mikolášek, P. Pribytný, D. Donoval, J. Marek, A. Chvála, M. Molnár, and J. Kováč, “Suppression of interface recombination by buffer layer for back contacted silicon heterojunction solar cells”, in 8th Solid State Surfaces and Interfaces, vol. 312, September 2014, pp. 145–151
- [10] M. Schmidt, L. Korte, a Laades, R. Stangl, C. Schubert, H. Angermann, E. Conrad, and K. Maydell, “Physical aspects of a-Si:H/c-Si heterojunction solar cells,” Thin Solid Films, vol. 515, no. 19, pp. 7475–7480, 2007.
- [11] H. Angermann, L. Korte, J. Rappich, E. Conrad, I. Sieber, M. Schmidt, K. Hubener, and J. Hauschild, “Optimisation of electronic interface properties of a-Si:H/c-Si hetero-junction solar cells by wet-chemical surface pre-treatment,” Thin Solid Films, vol. 516, no. 20, pp. 6775–6781, 2008.
- [12] H. Angermann, “Passivation of structured p-type silicon interfaces: Effect of surface morphology and wet-chemical pre-treatment,” Appl. Surf. Sci., vol. 254, no. 24, pp. 8067–8074, 2008.
- [13] M. Mikolášek, E. Stuchliková, L. Harmatha, A. Vincze, M. Nemeč, J. Racko, J. Breza, “Capacitance study of carrier inversion at the amorphous/crystalline silicon heterojunction passivated by different thicknesses of i-layer”, Appl. Surf. Sci., 312 (2014), pp. 152–156.